Environmental Health Perspectives
Vol. 54, pp. 93–103, 1984

Structure of Mammalian Metallothionein

by Jeremias H. R. Kägi,* Milan Vašák,* Konrad Lerch,* David E. O. Gilg,* Peter Hunziker,* Werner R. Bernhard* and Meinrad Good*

All mammalian metallothioneins characterized contain a single polypeptide chain of 61 amino acid residues, among them 20 cysteines providing the ligands for seven metal-binding sites. Native metallothioneins are usually heterogeneous in metal composition, with Zn, Cd, and Cu occurring in varying proportions. However, forms containing only a single metal species, i.e., Zn, Cd, Ni, Co, Hg, Pb, Bi, have now been prepared by *in vitro* reconstitution from the metal-free apoprotein. By spectroscopic analysis of such derivatives it was established that all cysteine residues participate in metal binding, that each metal ion is bound to four thiolate ligands, and that the symmetry of each complex is close to that of a tetrahedron.

To satisfy the requirements of the overall $Me_7(Cys^-)_{20}$ stoichiometry, the complexes must be combined to form metal–thiolate cluster structures. Experimental proof for the occurrence of such clusters comes from the demonstration of metal–metal interactions by spectroscopic and magnetic means. Thus, in $Co(II)_7$-metallothionein, the Co(II)-specific ESR signals are effectively suppressed by antiferromagnetic coupling of juxtaposed paramagnetic metal ions. By monitoring changes in ESR signal size occurring on stepwise incorporation of Co(II) into the protein, it is possible to follow the building up of the clusters. This process is biphasic. Up to binding of four equivalents of Co(II), the ESR amplitude increases in proportion to the metal content, indicating generation of magnetically noninteracting high-spin complexes. However, upon addition of the remaining three equivalents of Co(II), these features are progressively suppressed, signaling the formation of clusters. The same mode of cluster formation has also been documented for Cd and Hg.

The actual spatial organization of the clusters and the polypeptide chain remains to be established. An attractive possibility is the arrangement of the tetrahedral metal–thiolates in adamantane-like structures surrounded by properly folded segments of the chain providing the ligands. ^{1}H-NMR data and infrared absorption measurements are consistent with a tightly folded structure rich in β-type conformation.

Historically, it was in human kidney that the Russian geochemist D. P. Malyuga first serendipitously discovered the natural accumulation of cadmium in vertebrate tissues (*1*). Based on this observation, Margoshes and Vallee then proceeded to isolate from equine kidney the first cadmium-containing protein (*2*). This material, subsequently named metallothionein (3), was characterized by the following features (4): molecular weight 6000–7000; high metal content; characteristic amino acid composition (high cysteine content, no aromatic amino acids); unique distribution of cysteinyl residues in the amino acid sequence; optical features characteristic of metal thiolates.

At the First International Meeting on Metallothionein and Other Low Molecular Weight Metal-Binding Proteins in 1978 (*5*), the definition was adopted that any protein resembling equine renal metallothionein in several of these criteria can be classified as a metallothionein. Proteins satisfying this liberal definition have now been found to occur not only in many animal species but also in certain eukaryotic microorganisms (*6–8*), in some plants (*9,10*), and even in prokaryotes (*11,12*).

Table 1 lists the species and tissues in which the natural occurrence of metallothionein has been demonstrated and for which data on metal

*Biochemisches Institute der Universität Zürich, Winterthurerstrasse 190, CH-8057 Zürich, Switzerland.

composition are available. The variability in the proportions of the different group-2B metal ions and copper has been a unique and unorthodox feature of these proteins since the earliest reports (*2,3*). Clearly, there is no evidence either for a stoichiometric partitioning among the metals or for the existence of metal-specific sites. In fact, the occupation of the binding sites by a given metal seems to be determined not so much by the chemical affinity of the sites as by the supply of the metal and by biological variables, such as the tissue of origin (*13,14*), age, stage of development (*15*), and the activity of certain still poorly understood homeostatic mechanisms (*16*). While zinc is the more abundant component in nearly all mammals examined, copper tends to be more prevalent in fish. Thus, the patent variability in metal composition alone should guard against the assignment of a function of metallothionein with respect to a single metal. Most likely, the very broad metal-binding specificity provides for a multiplicity of biological roles that metallothionein may have acquired during evolution (Table 1).

Many metallothioneins are related to one another in their primary structure as documented by amino acid sequence analysis. Figure 1 summarizes most of the structural information available of what we propose to designate as class I metallothioneins. In addition to all mammalian metallothioneins thus far characterized, this class includes proteins from a fish (*Pleuronectes platessa*), a marine crab (*Scylla serrata*) and from a mold (*Neurospora crassa*). The average 42% identity between the aligned sequences of the arthropode and mammalian forms and the average 32% identity between Neurospora metallothionein and the corresponding *N*-terminal segment of all other metallothioneins included in the comparison leave no doubt about a common origin of the genes coding for them. With the limited number of sequences available it is, of course, premature to attempt the construction of a phylogenetic tree. However, from the manifest differences between the sequences of metallothioneins of phyla whose separation in evolution can be dated, it is feasible to obtain an estimate of the average rate of evolution of this class of proteins. The time course of the emergence of structural changes expressed in percent difference of the aligned segments of pairs of sequences is shown in Figure 2. After correcting for back mutations (*45*) and by assuming that separation of vertebrates and invertebrates occurred some 600 million years ago, one calculates from the comparison of the crab metallothioneins with all mammalian forms an average rate of 7.2×10^{-10} amino acid substitutions per year corresponding

Table 1. Occurrence and metal composition of metallothionein.[a]

Species	Organ	Metal composition				Reference
		Zn	Cd	Cu	Hg	
Man	Liver	+ + + + + +	±	±	−	(*17*)
	Kidney	+ + +	+ + +	+	±	(*18*)
	Fetal liver	+ + + +		+ +		(*19*)
	Neonatal liver	+ + + +		+ +		(*15*)
Horse	Liver	+ + + + +	+	±		(*20*)
	Kidney	+ + +	+ + +	±		(*21*)
	Intestine	+ + + +	+ +	±		(*22*)
Sea lion	Kidney	+ + +			+ + +	(*23*)
Sheep	Fetal liver	+ + + +		+ +		(*24*)
Pig	Liver	+ + + +		+ +		(*25*)
Rabbit	Neonatal liver	+ + . + +		+		(*15*)
Syrian hamster	Neonatal liver	+ +		+ + + +		(*15*)
Chinese hamster	Neonatal liver	+ + + +		+ +		(*15*)
Rat	Neonatal liver	+ + + + +		+		(*26*)
	Neonatal kidney	+ + + + +		+		(*27*)
	Adult liver	+ + + +		+ +		(*22*)
	Adult kidney	+ +		+ + + +		(*27*)
	Adult testes	+ + + + +		+		(*27*)
Mouse	Neonatal liver	+ + +		+ + +		(*15*)
Duck	Liver	+ +	+	+ + +		(*28*)
Flounder	Liver	+	±	+ + + + +		(*29*)
Skipjack	Liver	+	+ + +	+ + +		(*30*)
Eel	Liver	+ + +	±	+ + +		(*31*)
Crab	Hepatopancreas	±	+ + +	+ + +		(*32*)
Limpet	Soft tissue	+ + +	+ +	+		(*33*)

[a]All data refer to metallothionein obtained from organisms not subjected to experimental pretreatment with metals.

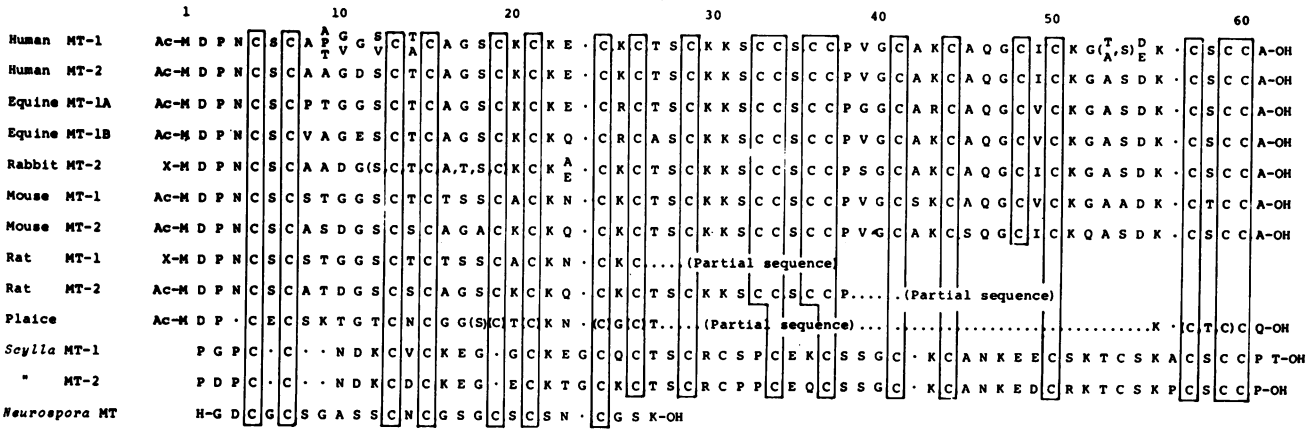

FIGURE 1. Amino acid sequences of class I metallothioneins (MT). The sequences were taken from the following references given in parentheses: human MT-1 (*34*), human MT-2 (*35*), equine MT-1A (*13*), equine MT-1B (*34*), rabbit MT-2 (*37*), mouse MT-1 (*38*), mouse MT-2 (*39*), rat MT-1 (*40*), rat MT-2 (*41*), plaice MT (*42*), scylla MT-1 and MT-2 (*43*), Neurospora MT (*6*). The numeration refers to the sequence of mammalian metallothioneins. The residues enclosed within parentheses require further identification. Dots between adjacent residues denote deletions introduced for optimal alignment. Residues 58 and 59 of the human and equine metallothioneins were reassigned following sequence reexamination (M. Kimura and J. H. R. Kägi, unpublished data). Residue 23 of mouse metallothionein-1 was reassigned on the basis of the cDNA sequence (*44*).

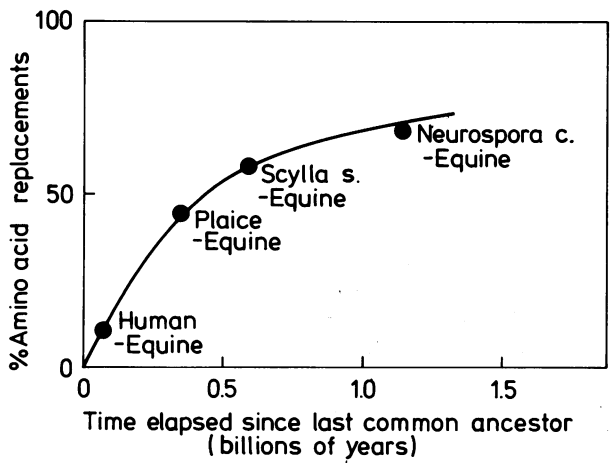

FIGURE 2. Evolution of class I metallothioneins. Relation of number of variant residues among class I metallothioneins from organisms of different classes and phyla to the time elapsed since the divergence of the corresponding lines of evolutionary descent. In each comparison the reference protein is equine metallothionein-1B.

Table 2. Rate of molecular evolution of class I metallothioneins.

	Substitutions/codon/year
Histone IV	0.1×10^{-10}
Insulin A and B	3.3×10^{-10}
Cytochrome c	4.2×10^{-10}
Metallothionein	7.2×10^{-10}[a]
Hemoglobin α-chain	9.9×10^{-10}
Ribonuclease	25.3×10^{-10}
Fibrinopeptide A	42.9×10^{-10}

[a]Calculated from differences between mammalian and anthropode metallothioneins by the procedure of King and Jukes (*46*). The figures included for comparison were taken from the same reference.

to a unit evolutionary period of about 14 million years. A similar figure is obtained by comparing the Neurospora protein with all other metallothioneins. They range between those calculated previously for the globins and for cytochrome c, suggesting that class I metallothioneins are rather slowly evolving proteins (Table 2).

The sequencing studies have also established that mammalian metallothioneins display very substantial genetic polymorphism. There are two isometallothioneins in rodents (*47*) and there are at least four in horse (*13*) and in rabbit (*48*). An even larger multiplicity of forms exists in human tissues where not less than 11 genes or pseudogenes coding for metallothionein have been reported (*49*). The structural divergence of the isoproteins ranges from 1 to 15 amino acid substitutions, indicating that they must have arisen at various times during evolution. While isoproteins differing in electric charge can be isolated by electrophoretic techniques or by ion-exchange chromatography (*5,50*), many isoforms are not resolved by these methods. A remarkably good resolution of many isoproteins can be obtained, however, by reversed-phase HPLC

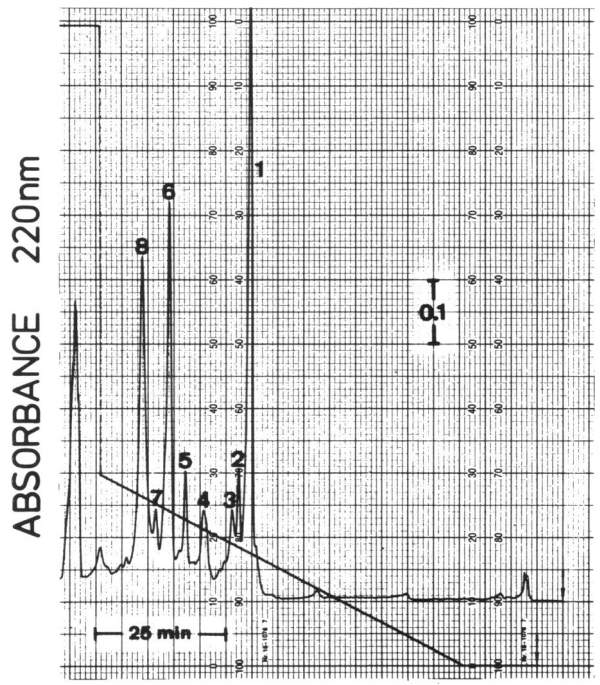

FIGURE 3. Polymorphism of metallothionein. Metallothionein isoprotein HPLC patterns from crude extract of human liver. Crude metallothionein (5 mg) prepared by gel filtration (*20*) was taken up in 0.5 mL 0.02 M Tris-HCl and chromatographed on semipreparative LiChrosorb RP 18 (10 μm) using a linear acetonitrile gradient (straight line) in 0.05 M Tris-HCl, pH 7.5, at a flow rate of 2 mL/min. Isometallothioneins were identified by amino acid analysis in the following peaks: 1 (MT-2), 3 (MT-1A), 5 (MT-1B), 6 (MT-1C) and 8 (MT-1D). Peak 2, 4 and 7 were not identified (*51*).

(*48,51*). As shown in Figure 3, it is now possible to separate in a single step five of the isometallothioneins present in the supernatant of human liver.

The chemically most significant information derived from comparative sequence analysis pertains to the mode in which the polypeptide chains provide for metal binding. The essential conditioning factor for metal complexation are the 20 cysteine residues whose position is completely preserved in all mammalian sequences known thus far (Fig. 4). The most unique feature is the repetitive occurrence of the cys-x-cys- tripeptide sequence, where x usually stands for a residue other than cysteine. Occurring seven times along the chain, these sequences have been suggested to serve as primary chelation sites for the seven group–2B metal ions usually bound to this protein and are thought to be essential for the formation of the metal–thiolate clusters typical of this protein (*vide infra*).

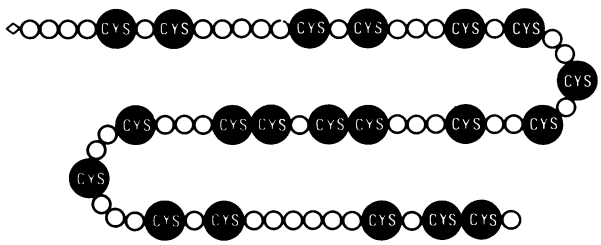

FIGURE 4. Mode of distribution of cysteine residues in mammalian metallothioneins (*4*).

That the metal ions are coordinated to the sulfur group of the cysteine residues was inferred early from the observation that native metallothionein contains no free sulfhydryl groups (*21*). All 20 cysteine residues are deprotonated, and hence they must occur as thiolate ligands bound to the seven bivalent metal ions, yielding the rather unusual stoichiometry of about three thiolate ligands per metal. This mode of metal binding entails the generation of an extra negative charge at six of the seven metal centers, thereby bringing about the overall negative charge typical of all metallothioneins on record (*5,52*).

The earliest direct evidence for binding of the metal to cysteine sulfur was obtained from the electronic absorption spectrum of Cd(II)-containing forms of metallothionein which is characterized by a broad absorption shoulder at 250 nm superimposed upon protein absorption (*21,53*). The same feature occurs in Cd(II)-complexes of 2-mercaptoethanol (*53*) and of synthetic peptides containing the cys-x-cys sequence (*54*). It disappeared completely upon removal of the metal at low pH, and hence it was attributed to a ligand-metal electron transfer transition (*21,53*). This assignment is also supported by a recent comparative spectroscopic study of a series of monosubstituted derivatives of metallothionein containing a full complement of Zn(II), Cd(II), Hg(II), Pb(II), and Bi(III) (*55*). The striking features of these spectra (Fig. 5) are the strong metal-induced absorption envelopes and the large red shift which increases on going from the lighter to the heavier metals.

According to the semiempirical theory of Jørgensen (*56*), the spectral location ($\tilde{\nu}$) of the lowest energy electron transfer band of such metal complexes is a simple function of the difference in optical electronegativity of the ligand χ_{opt} (L) and of the metal χ_{opt} (M) as given by the expression

$$\tilde{\nu}\ (\mu m^{-1}) = (3.0\ \mu m^{-1})\ [\chi_{opt}(L) - \chi_{opt}(M)]$$

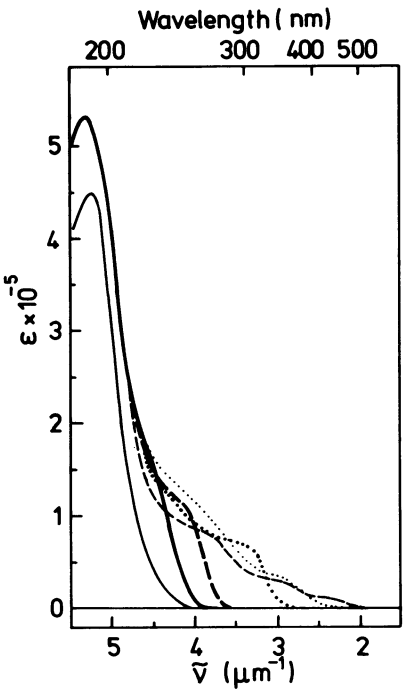

FIGURE 5. UV absorption spectra of (——) apometallothionein at pH 2, and of metallothionein at pH 8 containing a full complement (7 moles per mole) of (—) zinc, (--) cadmium (• • •) mercury, (--) bismuth and (· · ·) lead (*55*).

Table 3. Location of first metal-thiolate electron transfer transition in monosubstituted metal derivatives of metallothionein (MT).

	Observed		Calculated[1]	
Derivative	μm⁻¹	(nm)	μm⁻¹	(nm)
$Zn(II)_7$-MT	4.33	(231)	4.31	(232)
$Cd(II)_7$-MT	4.00	(250)	4.01	(249)
$Hg(II)_7$-MT	3.25	(308)	3.21	(312)
$Pb(II)_7$-MT	2.50	(400)	2.49	(401)

[1]Calculated from the difference of the optical electronegativities of the bonded atoms (*56*). The values for the optical electronegativities employed were 2.6 for thiolate (RS^-), 1.15 for Zn(II), 1.27 for Cd(II), 1.50 for Hg(II) and 1.77 for Pb(II). The values for the metals were deduced from absorption spectra for tetrahedral halide complexes (*61,62*).

The values of the optical electronegativities are determined by the chemical nature and the coordination geometry of the complexes and can be obtained from the spectra of model complexes. That this theory holds for metallothionein is documented in Table 3, where the predicted positions of these bands calculated for tetrahedral model complexes of Zn(II), Cd(II), Hg(II), and Pb(II) with thiolate ligands are compared with the actual location of the first electron transfer transitions in the absorption spectra of the corresponding monosubstituted metallothioneins. The excellent agreement between the two sets of data strongly suggests that in metallothionein the metal ions are bound in tetrahedral geometry and that each of the seven metal ions is surrounded by four cysteine residues. Identical inferences have also been drawn from spectroscopic studies of $Co(II)_7$-metallothionein (*57*).

Since the protein contains 20 cysteine residues and usually binds seven bivalent metal ions, it follows from these spectroscopic data that the options for the accommodation of the metal ions are severely restricted. Clearly, there are not enough cysteines to provide every metal ion with four separate thiolate ligands, and hence there must be a sharing of some of these ligands by adjacent metal ions giving rise to the formation of metal–thiolate cluster complexes. The observed stoichiometry dictates that the 20 cysteine residues present in the molecule must be partitioned into eight doubly coordinated bridging thiolate ligands and twelve singly coordinated terminal thiolate ligands.

The first direct evidence for the existence of metal–thiolate clusters in metallothionein came from the ^{113}Cd-NMR studies of Otvos and Armitage (*59*), who deduced from homonuclear decoupling measurements that the protein contains two separate metal–thiolate clusters, one with three and one with four metal ions, respectively. Similar conclusions are also obtained from spectroscopic and magnetic studies of Co(II)-substituted metallothionein (*60*). Co(II) has chemical properties similar to those of Zn(II). Therefore, this metal can replace zinc in many metalloproteins including metallothionein. Due to its transition-metal nature, the introduction of Co(II) into metallothionein produces an emerald-green derivative whose absorption spectrum offers proof that the metal is bound tetrahedrally to four thiolate ligands (Fig. 6).

Because Co(II) has unpaired electrons it can also serve as a paramagnetic probe of its molecular environment. Accordingly, Co(II) can sense the presence of other Co(II) ions when they occur in close proximity, i.e., in a cluster complex. Such Co(II)–Co(II) interactions manifest themselves mainly by intensity changes in the electron spin resonance (ESR) properties. The ESR spectrum of Co(II)–metallothionein shown in Figure 7, (left), is typical of high-spin Co(II) as expected for tetrahedral complexes. The same profile is also seen in partially saturated Co(II)–metallothionein, but its intensity monitored by the amplitude of the major signal at 1000 Gauss ($g_x \sim 5.9$) shows an

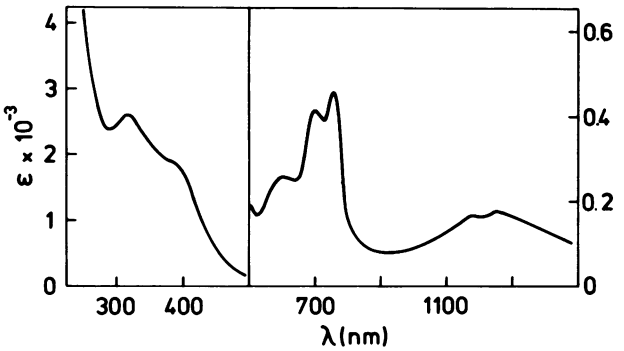

FIGURE 6. Absorption spectrum of rabbit liver Co(II)$_7$-metallothionein in 0.05 M Tris-HCl, pH 7. The molar absorbancy refers to the metal (*58*).

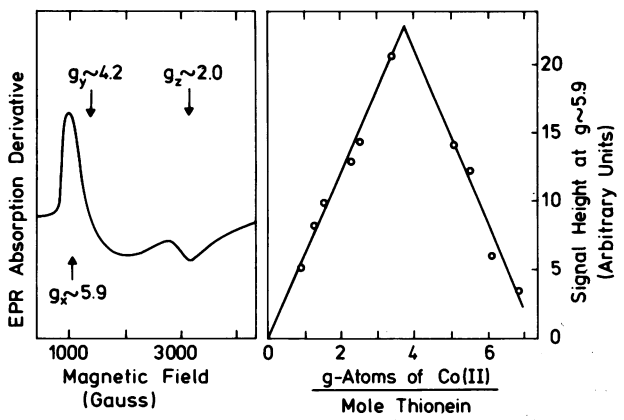

FIGURE 7. Electron spin resonance (ESR) titration of rabbit liver apometallothionein with Co(II): (left) ESR spectrum of Co(II)$_7$-metallothionein at 4°K, (right) dependency of ESR signal height at $g_x \approx 5.9$ on Co(II)-to-protein ratio (*60*).

unusual dependence on metal-to-protein stoichiometry. On titration of the metal-free protein (apometallothionein) with Co(II) (Fig. 7, right), the signal increases at first in proportion to the paramagnetic metal ion added. However, this trend changes abruptly after incorporation of nearly four Co(II). On further addition of Co(II) there is a progressive loss of signal, yielding an ESR spectrum of the fully reconstituted derivative that has an even lower amplitude than that recorded after adding only 1 mole of Co(II). The explanation for this anomalous titration behavior is spin canceling due to antiferromagnetic coupling of vicinal paramagnetic Co(II)-centers. Hence, together with magnetic susceptibility measurements (*60*), these data establish unambiguously that in Co(II)–metallothionein the metal ions are linked in one or more oligonuclear clusters. The remarkably sharp transition from the paramagnetic nonclustered to the diamagnetic clustered structure upon filling up of the metal-binding sites of metallothionein indicates that under the conditions employed magnetically noninteracting complexes are formed first and, hence, that they must be energetically more stable than the clustered complexes. The same noncooperative mode of binding in which spatially segregated metal complexes are formed before the clusters are completed was recently observed also in the formation of Cd$_7$–metallothionein (*54*) and of Hg$_7$–metallothionein (*55*).

The cluster model fitting the observed spectroscopic features best is the adamantane-like metal–thiolate cage depicted in Figure 8. This decahedron first proposed by Dance on the basis of crystallographic studies of synthetic model compounds (*63,64*) is similar to the structures inferred from the ^{113}Cd-NMR studies (*59*). Its attractive feature is that it fully preserves the tetrahedral coordination of each metal ion while allowing their interconnection through thiolate ligands. Its occurrence in metallothionein, albeit in a somewhat modified form, affords a ready explanation for the remarkable simplicity of the electronic spectra discussed above. The adamantane model also illustrates nicely the partitioning of the sulfur ligands into two classes, the bridging thiolates together with the metal forming the decahedron, and the terminal thiolates located outside the polyhedral cage. The model implies that the cluster is located in the interior of the protein surrounded by the segments of the polypeptide chain providing the ligands.

Although some estimates of the gross physical features of metallothionein have been made from hydrodynamic measurements (*20*) and although there is now good evidence that the two metal–

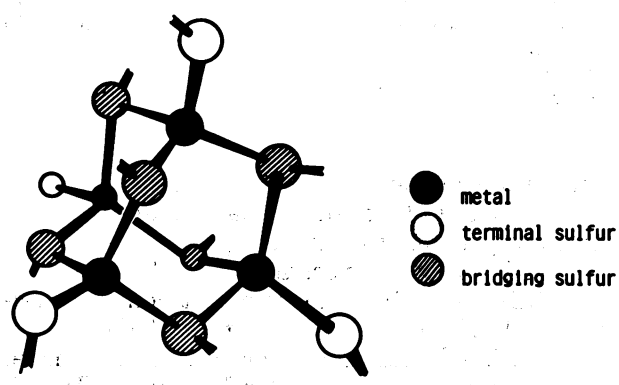

FIGURE 8. Adamantane-type metal–thiolate cluster proposed for metallothionein.

thiolate clusters inferred from ^{113}Cd-NMR studies (*59*) are located in the N- and C-terminal domains of the protein, respectively (*65*), little detailed documentation is as yet available on the spatial organization of this protein (*66*). Techniques sensitive to polypeptide conformation such as circular dichroism, infrared absorption spectroscopy, and ^{1}H–NMR spectroscopy have, however, given some information on protein folding both in the metal-free and in the metal-containing forms.

Representative far-UV circular dichroism spectra of the two forms are shown in Figure 9. Both spectra display the strongest ellipticity band at about 200 nm, suggesting a large proportion of disordered structure (*67*). At longer wavelengths, there are, however, substantial differences which can in part arise from differences in polypeptide folding (*vide infra*) but which to an appreciable extent are also the result of the superposition of ellipticity contributions of the Zn(II)–thiolate chromophore upon the circular dichroism of the apoprotein. Accordingly, secondary structure analysis by computer fitting of the circular dichroism spectrum using parameters derived from crystallographically defined proteins (*68*) is feasible only for the metal-free form. Table 4 shows the result of such a study carried out on equine liver metallothionein-1A. It suggests that the apoprotein still contains about 45% secondary structure, most of it as β-sheet and β-turn conformation. It is interesting that the figures obtained are in good agreement with the values calculated from the amino acid sequence using the secondary structure prediction method of Chou and Fasman (*69*).

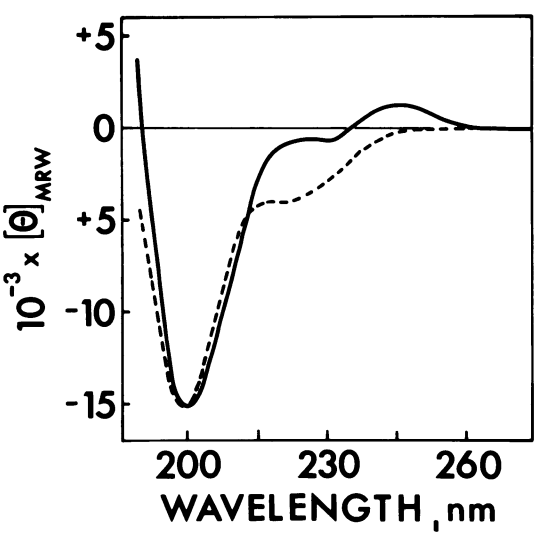

FIGURE 9. Circular dichroism spectra of (——) human liver Zn(II)-metallothionein (MT-2) in 0.05 M sodium phosphate buffer, pH 7.0; (– –) human apometallothionein in 0.02 M perchloric acid, pH 1.7 Ordinate: mean residue ellipticity ($[\Theta]_{MRW}$) refers to a mean residue weight of 99 (*67*).

Since tetrahedral binding of the seven metal ions to the 20 cysteine residues introduces not fewer than 42 additional crosslinks into the molecule, it is to be anticipated that metal complexation will impose new conformational constraints on the folding of the chain, bringing about some changes in secondary structure. This is, in fact, confirmed by a comparison of the metal-free and metal-containing forms of metallothionein by infrared absorption spectroscopy, a method which yields information on secondary structure folding. Over far-UV circular dichroism measurements it has the advantage of the conformation-dependent spectral features not being obscured by contributions from the metal–thiolate chromophores (Fig. 10). In this technique, position and shape of the amide I vibration near 1650 cm^{-1} are monitored in a solution of the protein in $^{2}H_2O$ (*70,71*). For comparison, spectra of deuterated reference proteins are also included. The predominantly α–helices containing myoglobin shows its amide I absorption maximum at 1650 cm^{-1} and β-structure-containing ribonuclease at 1639 cm^{-1}.

The disordered polypeptide conformation in proteins displays a maximum at about 1645 cm^{-1} and a weak shoulder at 1670 cm^{-1}. β-Structure produces both a maximum at 1634 cm^{-1} and a strong and a weak shoulder at 1660 and 1680 cm^{-1}, respectively. The maximum of apometallothionein is located at 1647 cm^{-1}, confirming the presence of a large proportion of disordered structure. The shape of the absorption band of the holoprotein is similar but the displacement of the amide I band to 1643 cm^{-1}, the intensification of the shoulder at 1660 cm^{-1}, and the increase in total amplitude are suggestive of an appreciable increase in β-structure content on metal binding (D. Gilg and J. H. R. Kägi, unpublished observation).

Table 4. Secondary structure analysis of equine liver metallothionein-1A.

Type	Secondary structure estimated from circular dichroism spectrum, %[a]	Secondary structure prediction from sequence, %[b]
α-Helix	6	10
β-Sheet	18	16
β-Turn	21	26
Disordered structure	55	48

[a]Evaluated according to Provencher and Glöckner (*68*).
[b]Calculated according to Chou and Fasman (*69*).

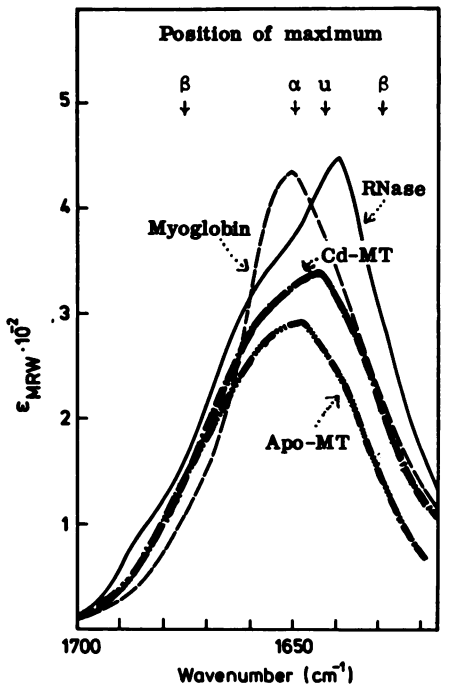

FIGURE 10. Amide I region in IR spectra of apometallothionein-2 (apo-MT) at pH 1.6, and of metallothionein (Cd-MT), myoglobin and ribonuclease (RNase) at pH 7.5. All spectra are recorded in ^2H_2O. The vertical arrows indicate the positions of the maxima of protein amide I transitions typical for pleated sheet (β), α-helix (α) and unordered (u) conformations in ^2H_2O (*72*).

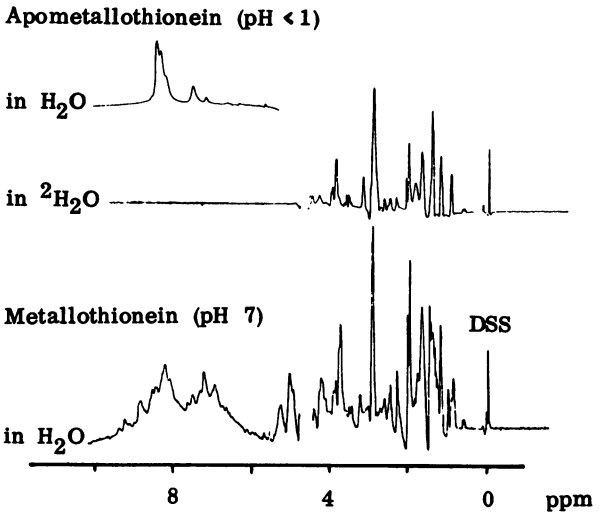

FIGURE 11. 270-MHz ^{1}H-NMR spectra of (bottom) equine metallothionein-1A and (top) apometallothionein. To obtain the spectra in H_2O, the solvent signal was suppressed by a gated pulse (*75*).

The stabilizing influence of metal binding on the secondary and tertiary structure is further underscored by the early observation that unlike the metal-free protein (*65*), the metal-containing form is highly resistant to proteolysis (*73*), and that some of the peptide hydrogens are shielded from exchanging with the solvent (*74*). This is now also supported by comparative ^{1}H-NMR studies (*76*). The differences between the two forms are particularly striking in the low-field region (6.5–9.5 ppm), where only resonances of the secondary amide groups of the polypeptide chain and of the N-bound protons of the amino acid side chains occur (Fig. 11). While in the apoprotein in $^1H_20$ these resonances are collected to relatively narrow bands, in the metal-containing form they are spread over a chemical shift span of nearly 3 ppm, indicating substantial hydrogen bonding.

The structural differences are also manifest in the high-field region (0–4 ppm) (*75,77*). However, because of the absence of aromatic residues in the molecule and, hence, of aromatic ring current effects, shifts arising from changes in the environment of the protons are less pronounced and are difficult to interpret. These limitations inherent in one-dimensional ^{1}H-NMR spectra of proteins are now being overcome, however, by the application of two-dimensional ^{1}H-NMR techniques already applied successfully to a number of other systems (*78*). Studies on rabbit liver metallothionein currently conducted in collaboration with the Institute of Molecular Biology and Biophysics, ETH, Zürich, have led to the resolution of nearly all individual ^{1}H spin systems of the protein and have permitted sequential assignment of about 80% of the signals (*79*). It is anticipated that this technique, in conjunction with ^{1}H-^{113}Cd heteronuclear coupling studies, will provide a realistic spatial model of the folded molecule.

In conclusion, the chemical and spectroscopic data presented reflect the progress made in recent years in the understanding of the structure of this highly unusual protein. Among the major findings are (1) the remarkable conservation of the primary structure manifesting itself in the nearly complete invariance of the positions of the metal-binding cysteine residues and (2) the detailed knowledge gained from physical studies on the structural organization of the metal-binding sites, i.e., the unambiguous demonstration that bivalent metal ions are bound in tetrahedral microsymmetry to four thiolate ligands and that these complexes are joined to form discrete metal–thiolate clusters. These oligonuclear complexes constitute the first example of clusters of group–2B metal ions in a biological system. Their

unique occurrence in metallothionein implies that cluster formation with these bivalent metal ions is dependent on the very special distribution of cysteine residues characteristic for this protein. In fact, it seems most likely that it is the stringency of the stereochemical requirements for cluster formation that is responsible for the remarkable preservation of the positions of the cysteine residues in class I metallothionein throughout evolution.

The work was supported by Swiss National Science Foundation Grant No. 3.207-0.82 and the Kanton Zürich.

Dedicated to Professor F. Leuthardt, Zürich, on the occasion of his 80th birthday.

REFERENCES

1. Malyuga, D. P. On cadmium in organisms. Dokl. Akad. Nauk SSSR 31: 145–147 (1941).
2. Margoshes, M., and Vallee, B. L. A cadmium protein from equine kidney cortex. J. Am. Chem. Soc. 79: 4813–4814 (1957).
3. Kägi, J. H. R., and Vallee, B. L. Metallothionein: a cadmium- and zinc-containing protein from equine and renal cortex. J. Biol. Chem. 235: 3460–3465 (1960).
4. Kojima, Y., and Kägi, J. H. R. Metallothionein. Trends Biochem. Sci. 3: 90–93 (1978).
5. Nordberg, M., and Kojima, Y. Metallothionein and other low molecular weight metal-binding proteins. In: Metallothionein (J. H. R. Kägi and M. Nordberg, Eds.), Birkhäuser Verlag, Basel, 1979, pp. 41–135.
6. Lerch, K. Amino-acid sequence of copper-metallothionein from *Neurospora crassa*. In: Metallothionein (J. H. R. Kägi and M. Nordberg, Eds.), Birkhäuser Verlag, Basel, 1979, pp. 173–179.
7. Prinz, R., and Weser, U. A naturally occurring Cu-thionein in *Saccharomyces cerevisiae*. Hoppe-Seyler's Z. Physiol. Chem. 356: 767–776 (1975).
8. Nakamura, Y., Katayama, S., Okada, Y., Suzuki, F., and Nagata, Y. The isolation and characterization of a cadmium- and zinc-binding protein from *Tetrahymena pyriformis*. Agr. Biol. Chem. 45: 1167–1172 (1981).
9. Rauser, W. E., and Curvetto, N. R. Metallothionein occurs in roots of *Agrostis* tolerant to excess copper. Nature 287: 563–564 (1980).
10. Bartolf, M., Brennan, E., and Price, C. A. Partial characterization of a cadmium-binding protein from the roots of cadmium-treated tomato. Plant Physiol. 66: 438–441 (1980).
11. Maclean, F. I., Lucis, O. J., Shaikh, Z. A., and Jansz, E. R. The uptake and subcellular distribution of Cd and Zn in microorganisms. Fed. Proc. 31: 699 (1972).
12. Higham, D. P., and Sadler, P. J. Bacterial cadmium-binding proteins. Inorg. Chim. Acta 79: 140–142 (1983).
13. Kojima, Y., Berger, C., and Kägi, J. H. R. The amino acid sequence of equine metallothioneins. In: Metallothionein (J. H. R. Kägi and M. Nordberg, Eds.), Birkhäuser Verlag, Basel, 1979, pp. 153–161.
14. Zelazowski, A. J., and Szymańska, J. A. Low molecular weight cadmium- and copper-binding proteins from rat kidneys. Biol. Trace Elem. Res. 2: 137–148 (1980).
15. Bakka, A., and Webb, M. Metabolism of zinc and copper in the neonate: changes in the concentrations and contents of thionein-bound Zn and Cu with age in the livers of the newborn of various mammalian species. Biochem. Pharmacol. 30: 721–725 (1981).
16. Ohtake, H., and Koga, M. Purification and characterization of zinc-binding protein from the liver of the partially hepatectomized rat. Biochem. J. 183: 683–690 (1979).
17. Bühler, R. H. O., and Kägi, J. H. R. Human hepatic metallothioneins. FEBS Letters 39: 229–234 (1974).
18. Pulido, P., Kägi, J. H. R., and Vallee, B. L. Isolation and some properties of human metallothionein. Biochemistry 5: 1768–1777 (1966).
19. Riordan, J. R., and Richards, V. Human fetal liver contains both zinc- and copper-rich forms of metallothionein. J. Biol. Chem. 255: 5380–5383 (1980).
20. Kägi, J. H. R., Himmelhoch, S. R., Whanger, P. D., Bethune, J. L., and Vallee, B. L. Equine hepatic and renal metallothioneins. Purification, molecular weight, amino acid composition, and metal content. J. Biol. Chem. 249: 3537–3542 (1974).
21. Kägi, J. H. R., and Vallee, B. L. Metallothionein: a cadmium- and zinc-containing protein from equine renal cortex. II. Physicochemical properties. J. Biol. Chem. 236: 2435–2442 (1961).
22. Kägi, J. H. R., Kojima, Y., Berger, C., Kissling, M. M., Lerch, K., and Vašák, M. Metallothionein: structure and evolution. In: Metalloproteins (U. Weser, Ed.), Georg Thieme Verlag, Stuttgart, 1979, pp. 194–206.
23. Lee, S. S., Mate, B. R., von der Trenck, K. T., Rimerman, R. A., and Bühler, D. R. Metallothionein and the subcellular localization of mercury and cadmium in the California sea lion. Comp. Biochem. Physiol. 57C: 45–53 (1977).
24. Bremner, I., Williams, R. B., and Young, B. W. Distribution of copper and zinc in the liver of the developing sheep foetus. Brit. J. Nutr. 38: 87–92 (1977).
25. Bremner, I. The relationship between the zinc status of pigs and the occurrence of copper- and Zn-binding proteins in liver. Brit. J. Nutr. 35: 245–252 (1976).
26. Mason, R., Bakka, A., Samarawickrama, G. P., and Webb, M. Metabolism of zinc and copper in the neonate: accumulation and function of (Zn, Cu)-metallothionein in the liver of the newborn rat. Brit. J. Nutr. 45: 375–389 (1980).
27. Brady, F. O., and Webb, M. Metabolism of zinc and copper in the neonate. J. Biol. Chem. 256: 3931–3935 (1981).
28. Brown, D. A., Bawden, C. A., Chatel, K. W., and Parsons, T. R. The wildlife community of Iona Island Jetty, Vancouver, B.C., and heavy-metal pollution effects. Environ. Conserv. 4: 213–216 (1977).
29. Brown, D. A. Increases of Cd and the Cd:Zn ratio in the high molecular weight protein pool from apparently normal liver of tumor-bearing flounders *(Parophrys vetulus)*. Mar. Biol. 44: 203–209 (1977).
30. Takeda, H., and Shimizu, C. Purification of metallothionein from the liver of skipjack and its properties. Nippon Suisan Gakkaishi 48: 717–723 (1982).
31. Noël-Lambot, F., Gerday, C., and Distèche, A. Distribution of Cd, Zn, and Cu in liver and gills of the eel *Anguilla anguilla* with special reference to metallothioneins. Comp. Biochem. Physiol. 61C: 177–187 (1978).
32. Overnell, J., and Trewhella, E. Evidence for the natural occurrence of (cadmium, copper)-metallothionein in the crab *Cancer pagurus*. Comp. Biochem. Physiol. 64C: 69–76 (1979).
33. Howard, A. G., and Nickless, G. Protein binding of cadmium, zinc and copper in environmentally insulted limpets *Patella vulgata*. J. Chromat. 104: 457–459 (1975).
34. Kissling, M. M., and Kägi, J. H. R. Amino acid sequence of human hepatic metallothioneins. In: Metallothionein

(J. H. R. Kägi and M. Nordberg, Eds.), Birkhäuser Verlag, Basel, 1979, pp. 145–151.
35. Kissling, M. M., and Kägi, J. H. R. Primary structure of human hepatic metallothioneins. FEBS Letters 82: 247–250 (1977).
36. Kojima, Y., Berger, C., Vallee, B. L., and Kägi, J. H. R. Amino-acid sequence of equine renal metallothionein-1B. Proc. Natl. Acad. Sci. (U.S.) 73: 3413–3417 (1976).
37. Kimura, M., Otaki, N., and Imano, M. Rabbit liver metallothionein. Tentative amino acid sequence of metallothionein-B. In: Metallothionein (J. H. R. Kägi and M. Nordberg, Eds.), Birkhäuser Verlag, Basel, 1979, pp. 163–168.
38. Huang, I.-Y., Yoshida, A., Tsunoo, H., and Nakajima, H. Mouse liver metallothioneins. Complete amino acid sequence of metallothionein-I. J. Biol. Chem. 252: 8217–8221 (1977).
39. Huang, I.-Y., Kimura, M., Hata, A., Tsunoo, H., and Yoshida, A. Complete amino acid sequence of mouse liver metallothionein-II. J. Biochem. 89: 1839–1845 (1981).
40. Berger, C., Kissling, M. M., Andersen, R. D., Weser, U., and Kägi, J. H. R. Amino acid sequence of rat metallothioneins (MT) and of gene product of rat MT-mRNAs. Experientia 37: 619 (1981).
41. Kissling, M. M., Berger, C., Kägi, J. H. R., Andersen, R. D., and Weser, U. The amino-terminal sequence of a rat liver metallothionein (MT-2). In: Metallothionein (J. H. R. Kägi and M. Nordberg, Eds.), Birkhäuser Verlag, Basel, 1979, pp. 181–185.
42. Overnell, J., Berger, C., and Wilson, K. J. Partial amino acid sequence of metallothionein from the plaice (*Pleuronectes platessa*). Biochem. Soc. Trans. 9: 217–218 (1981).
43. Lerch, K., Ammer, D., and Olafson, R. W. Crab metallothionein. Primary structures of metallothioneins 1 and 2. J. Biol. Chem. 257: 2420–2426 (1982).
44. Mbikay, M., Maiti, I. B., and Thirion, J.-P. Cloning and sequencing of cDNA for mouse liver metallothionein-I. Biochem. Biophys. Res. Commun. 103: 825–832 (1981).
45. Margoliash, E., and Fitch, W. M. Evolutionary variability of cytochrome *c* primary structures. Ann. N.Y. Acad. Sci. 151: 359–381 (1968).
46. King, J. L., and Jukes, T. H. Non-Darwinian evolution. Science 164: 788–798 (1969).
47. Huang, I.-Y., Tsunoo, H., Kimura, M., Nakashima, H., and Yoshida, A. Primary structure of mouse liver metallothionein-I and -II. In: Metallothionein (J. H. R. Kägi and M. Nordberg, Eds.), Birkhäuser Verlag, Basel, 1979, pp. 169–172.
48. Klauser, S., Kägi, J. H. R., and Wilson, K. J. Characterization of isoprotein patterns in tissue extracts and isolated samples of metallothioneins by reverse-phase high-pressure liquid chromatography. Biochem. J. 209: 71–80 (1983).
49. Karin, M., and Richards, R. I. Human metallothionein genes—primary structure of the Metallothionein-II gene and a related processed gene. Nature 299: 797–802 (1982).
50. Suzuki, K. T. Direct connection of high-speed liquid chromatograph (equipped with gel permeation column) to atomic absorption spectrophotometer for metalloprotein analysis: metallothionein. Anal. Biochem. 102: 31–34 (1980).
51. Hunziker, P. E., and Kägi, J. H. R. Isolation of five human isometallothioneins. 15th Meeting of the Federation of European Biochemical Societies, Brussels, 1983, Abstracts, p. 217.
52. Bethune, J. L., Budreau, A. J., Kägi, J. H. R., and Vallee, B. L. Determination of the charge of horse kidney metallothionein by free boundary electrophoresis. In: Metallothionein (J. H. R. Kägi and M. Nordberg, Eds.), Birkhäuser Verlag, Basel, 1979, pp. 207–210.
53. Vašák, M. Kägi, J. H. R., and Hill, H. A. O. Zinc(II), cadmium(II), and mercury(II) thiolate transitions in metallothionein. Biochemistry 20: 2852–2856 (1981).
54. Willner, H., Vašák, M., and Kägi, J. H. R. Spectroscopic evidence for metal-thiolate clusters in complexes of Cd(II) with dithiol hexapeptides and in Cd-metallothionein. Inorg. Chim. Acta 79: 106 (1983).
55. Bernhard, W., Good, M., Vašák, M., and Kägi, J. H. R. Spectroscopic studies and characterization of metallothioneins containing mercury, lead and bismuth. Inorg. Chim. Acta 79: 154 (1983).
56. Jørgensen, C. K. Electron transfer spectra. Progr. Inorg. Chem. 12: 101–157 (1970).
57. Vašák, M., Kägi, J. H. R., Holmquist, B., and Vallee, B. L. Spectral studies of cobalt(II)- and nickel(II)-metallothionein. Biochemistry 20: 6659–6664 (1981).
58. Vašák, M., and Kägi, J. H. R. Mammalian metallothionein: evidence for metal thiolate clusters. In: Biomineralization and Biological Metal Accumulation (P. Westbroek and E. W. de Jong, Eds.), D. Reidel, Dordrecht, 1983, pp. 429–437.
59. Otvos, J. D., and Armitage, I. M. Structure of the metal clusters in rabbit liver metallothionein. Proc. Natl. Acad. Sci. (U.S.) 77: 7094–7098 (1980).
60. Vašák, M., and Kägi, J. H. R. Metal thiolate clusters in cobalt(II)-metallothionein. Proc. Natl. Acad. Sci. (U.S.) 78: 6709–6713 (1981).
61. Day, P., and Seal, R. H. Electronic spectra of some post-transition-metal halide complexes. J. Chem. Soc., Dalton Trans. 2054–2058 (1972).
62. Jørgensen, C. K. Inorganic Complexes. Academic Press, London, 1963.
63. Dance, I. G. Synthesis, crystal structure, and properties of the hexa(μ-benzenethiolato)tetra(benzenethiolatocobaltate(II)) dianion, the prototype cobalt(II)-thiolate molecular cluster. J. Am. Chem. Soc. 101: 6264–6273 (1979).
64. Dance, I. G. Formation, crystal structure, and reactions of catena-(μSPh) [$(\mu\text{-SPh})_6ZN_4(CH_3OH)(SPh)$], a model for zinc thiolate metalloenzymes. J. Am. Chem. Soc. 102: 3445–3451 (1980).
65. Winge, D. R., and Miklossy, K.-A. Domain nature of metallothionein. J. Biol. Chem. 257: 3471–3476 (1982).
66. Boulanger, Y., Goodman, C. M., Forte, C. P., Fesik, S. W., and Armitage, I. M. Model for mammalian metallothionein structure. Proc. Natl. Acad. Sci. (U.S.) 80: 1501–1505 (1983).
67. Bühler, R. H. O., and Kägi, J. H. R. Spectroscopic properties of zinc-metallothionein. In: Metallothionein (J. H. R. Kägi and M. Nordberg, Eds.), Birkhäuser Verlag, Basel, 1979, pp. 211–220.
68. Provencher, S. W., and Glöckner, J. Estimation of globular protein secondary structure from circular dichroism. Biochemistry 20: 33–37 (1981).
69. Chou, P. Y., and Fasman, G. D. Conformational parameters for amino acids in helical, β-sheet, and random coil regions calculated from proteins. Biochemistry 13: 211–222 (1974).
70. Cantor, C. R., and Timasheff, S. N. Optical spectroscopy of proteins. In: The Proteins (H. Neurath and R. L. Hill, Eds.), 3rd ed., Vol. V, Academic Press, New York, 1982, pp. 145–306.
71. Eckert, K., Grosse, R., Malur, J., and Repke, K. R. H. Calculation and use of protein-derived conformation-related spectra for the estimate of the secondary structure of proteins from their infrared spectra. Biopolymers 16: 2549–2563 (1977).

72. Vašák, M., and Kägi, J. H. R. Spectroscopic properties of metallothionein. In: Metal Ions in Biological Systems (H. Sigel, Ed.), Vol. 15, Marcel Dekker, New York, 1983, pp. 213–273.
73. Webb, M. Binding of cadmium ions by rat liver and kidney. Biochem. Pharmacol. 21: 2751–2765 (1972).
74. Ulmer, D. D., and Vallee, B. L. Structure and function of metalloenzymes. Adv. Chem. Ser. 100: 187–218 (1971).
75. Galdes, A., Vašák, M., Hill, H. A. O., and Kägi, J. H. R. ^{1}H NMR spectra of metallothioneins. FEBS Letters 92: 17–21 (1978).
76. Vašák, M., Galdes, A., Hill, H. A. O., Kägi, J. H. R., Bremmer, I., and Young, B. W. Investigation of the structure of metallothioneins by proton nuclear magnetic resonance spectroscopy. Biochemistry 19: 416–425 (1980).
77. Rupp, H., Voelter, W., and Weser, U. 270 MHz proton magnetic resonance spectra of metallothionein. FEBS Letters 40: 176–179 (1974).
78. Nagayama, K. Two-dimensional NMR spectroscopy: an application to the study of flexibility of protein molecules. Adv. Biophys. 14: 139–204 (1981).
79. Neuhaus, D., Wagner, G., Vašák, M., Kägi, J., and Wüthrich, K. Two-dimensional NMR studies of the conformation of metallothionein. VIth International Meeting on NMR Spectroscopy, Edinburgh, 1983, abstract.